Self-Association and Nitroaromatic-Induced Deaggregation of Pyrene Substituted Pyridine Amides

Sung Kuk Kim,[†] Jong Min Lim,[‡] Tuhin Pradhan,[§] Hyo Sung Jung,[§] Vincent M. Lynch,[†] Jong Seung Kim,*,[§] Dongho Kim,*,[‡] and Jonathan L. Sessler*,[†,‡]

[†]Department of Chemistry, The University of Texas at Austin, 105 East 24th Street, Stop A5300, Austin, Texas 78712-1224, United States

[‡]Department of Chemistry, Yonsei University, Seoul 120-749, Korea

[§]Department of Chemistry, Korea University, Seoul 136-701, Korea

Ⓢ *Supporting Information*

ABSTRACT: The self-assembly features of the bis-pyrene methyl amide functionalized pyridine and benzene "tweezers" **1** and **2** were studied in organic solution and in the solid state. These systems were found to display remarkably different self-association features and optical properties, which was rationalized by control experiments using compounds bearing pyrenemethyl esters, alkyl groups, or a single pyrene substituent (**3−6**). As dilute solutions in chloroform, tweezers **1** displays both pyrene monomer and excimer emission features reflecting intramolecular contacts between the pyrene subunits. At higher concentrations in chloroform, as well as in the solid state, tweezers **1** self-assembles to form a linear supramolecular polymer. In contrast, tweezers **2** does not interact in an intermolecular fashion and photoexcitation produces emission features characteristic of a pyrene monomer. DFT (density functional theory) and TDDFT (time dependent density functional theory) calculations revealed that the lowest vertical transitions are forbidden and that S_1 of **1** is an emissive state. In contrast to **1** and **2**, both pyrene-free control systems **5** and **6** were found to form linearly self-assembled supramolecular arrays in the solid state, albeit of differing structure. Upon exposure to trinitrobenzene (TNB), the self-assembled structures formed from **1** undergo deaggregation to form TNB complexes. This change is reflected in both an easily discernible color change and a quenching of the fluorescence emission intensity. Changes in the optical features were also seen in the case of **2**. However, notable differences between these two ostensibly similar systems were seen.
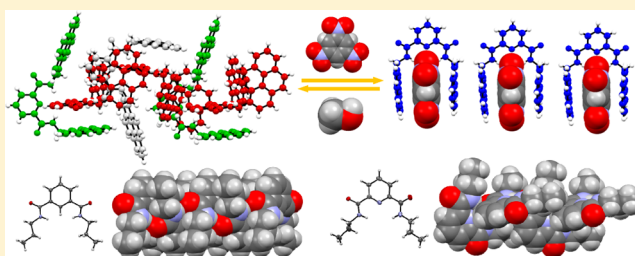
INTRODUCTION

Structurally defined cleft-like molecules containing two parallel subunits capable of interacting with substrates, so-called molecular tweezers, have received increasing attention over the years.[1] They have attracted interest for use in ion and small molecule recognition,[1a,b,d,f,h] in biomimetic chemistry,[1e,g] and as components of molecular machines,[1c] supramolecular polymers, and dendrimers.[1i] Early investigations by Zimmerman and co-workers established that rigid molecular tweezers based on electron rich acridine building blocks were able to bind the electron deficient guest 2,4,7-trinitrofluorenone within their open slot-like cavities.[2] More recently, Martín and co-workers reported that the molecular tweezers consisting of two extended tetrathiafulvalene (exTTF) units linked by a flexible spacer, such as an isophthalate, recognize C_{60} via electrostatic interactions involving the exTTF subunits and the relatively electron deficient fullerene.[3] In this case, the tweezers adjust their conformations so as to interact with the C_{60} guest via three different binding modes depending on the choice of solvent. In addition, the Martín group reported that molecular tweezers bearing both an electron donor and electron acceptors

on a central benzene core ring are capable of forming supramolecular polymers or dendrimers in highly concentrated solution.[4] These findings led us to consider that small variations in the structure of ostensibly similar molecular tweezers might have a significant impact on their ability to undergo self-assembly and to recognize targeted substrates. To test this hypothesis, we have sought to probe the recognition and self-assembly features of two structurally related bis-pyrene molecular tweezers, **1** and **2**, that contain central pyridine and benzene cores, respectively (see Chart 1). Also studied were control systems **3−6** (Chart 1) that bear pyrenemethyl esters or alkyl substituents, or contain only a single pyrene subunit. Compounds **1** and **2** are known compounds.[5] However, to the best of our knowledge, their self-assembly features have yet to be examined. Here, we report detailed optical, structural, and ^{1}H NMR spectroscopic studies of compounds **1** and **2** and detail the ability of **1** to form self-assembled structures in solution and in the solid state. We also

Chart 1. Structures of Compounds 1−6
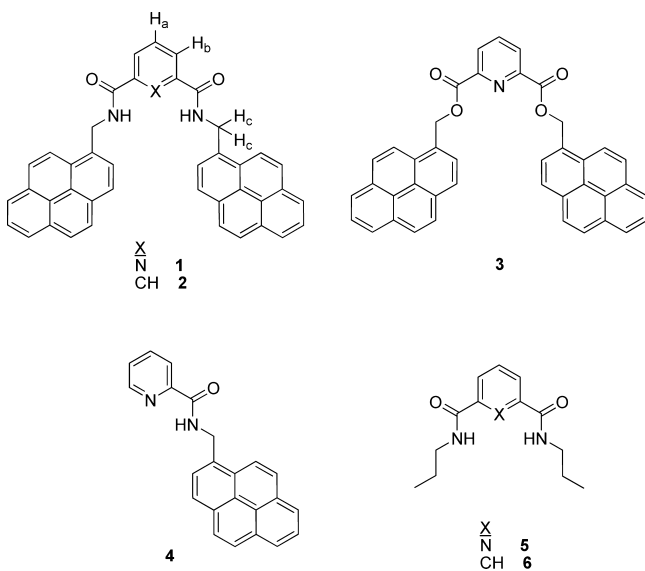
report the structural and optical changes that result from the recognition of trinitrobenzene (TNB) and trinitrotoluene (TNT).

Both **1** and **2** contain a pair of linking amide groups, a functionality that has been exploited extensively in the construction of self-assembled materials stabilized via intermolecular hydrogen bonding interactions.[6] However, as detailed further below, "tweezers" **1** and **2** were found to display remarkably different self-assembly and fluorescence emission features. These differences are further manifest in their interactions with electron deficient nitroaromatic explosives (NAEs). For instance, tweezers **1** self-associates to produce a linear oligomer both in chloroform solution and in the solid state; it also undergoes analyte-induced deaggregation when exposed to trinitrobenzene (TNB).[7−9] In contrast, no evidence of intermolecular interaction was found in the case of the phenyl-linked bis-pyrene tweezers compound **2**. Nor was it found to interact strongly with NAEs. The different behavior seen for compounds **1** and **2** is rationalized on the basis of a control experiment involving the pyrene-free systems **5** and **6**. Both compounds **5** and **6**, which contain pyridine and phenyl cores, respectively, undergo self-assembly to form linear supramolecular polymers albeit ones that differ in terms of their specific structures.

As detailed below, it was found that the small structural variation between tweezers **1** and **2** has a large impact on their optical properties, as well as their self-assembly characteristics, and their ability to bind electron deficient guests. For instance, whereas no evidence of appreciable excimer formation is seen in the phenyl linked tweezers **2**, the corresponding pyridine-linked congener **1** gives rise to characteristic pyrene excimer emission features in the fluorescence spectrum (i.e., λ_{max} = 470 nm) when subject to photoexcitation in chloroform at concentrations of ≤20 μM.[10a] On the basis of control studies involving **3−6** (vide infra), as well as dilution and solvent polarity studies, this excimer emission is thought to be intramolecular, as opposed to intermolecular, in origin and made possible as the result of internal amide−pyridine NH−N hydrogen bonds.[10b,c] Hydrogen bonding also plays a critical role in the aggregation seen for **1**, but not **2**. In the case of **1**, evidence for self-assembly is seen at higher concentrations

(≥0.5 mM) in CDCl$_3$ and in the solid state, as inferred from ^{1}H NMR spectroscopic measurements and a single crystal X-ray diffraction analysis, respectively.[11] These techniques were also used to study the TNB-triggered disassembly process and the nature of the resulting complex, **1·TNB**.

■ RESULTS AND DISCUSSION

Compounds **1** and **2** were recently reported by Colquhoun and co-workers as possible receptors for the recognition of specific sequences present on linear templates containing various chemical motifs.[5f,h] As part of this effort, the single crystal X-ray structure of compound **1** was solved. As published, the structure revealed a monomeric unit with nonparallel pyrene subunits.[5e] Our own examination of compound **1** led us to consider that the combined presence of two different types of aromatic subunits (pyridine and pyrene) and amide linkages would make it likely that this particular compound would undergo aggregation under conditions where hydrogen bonding or aromatic donor−acceptor interactions would be stabilized. Separate from these considerations, we envisioned that these same interactions could be modulated via the addition of electron deficient guests, such as TNB. To test this hypothesis, we have reprepared compound **1** and reanalyzed its X-ray structure. We have also prepared control compounds (**3−6**), including those containing pyrenemethyl esters, a single pyrene, or no pyrene at all. As detailed below, in the case of **1**, but not **2**, self-assembly takes place in the solid state and at typical NMR concentrations in CDCl$_3$. Moreover, in accord with our design expectations, exposure to test NAEs, such as TNB, leads to deaggregation and a considerable change in both the supramolecular structure and the fluorescence intensity.

The synthesis of compounds **1−6** is summarized in Schemes S1−S4 in the Supporting Information. Briefly, these systems were prepared via the simple reaction of pyrene methylamine hydrochloride, 1-pyrenemethanol, or propylamine with the requisite acid chloride in the presence of triethylamine or pyridine.

A single crystal of compound **1** suitable for single crystal X-ray diffraction analysis was obtained by subjecting **1** to slow evaporation from a mixture of chloroform and methanol. The resulting structure is shown in Figure 1. This structure reveals the presence of an ordered polymeric arrangement within the crystal lattice. This extended array is characterized by both close intermolecular amide−pyridine separations and short pyrene−pyridine and pyrene−pyrene contacts. Presumably, these close contacts reflect underlying stabilizing effects, including NH−N hydrogen bonds and π−π interactions. The net result is that in the solid state the ground state pyrene−pyrene contacts are exclusively intermolecular, rather than intramolecular, in nature. This is not true for the excited state interactions in solution (vide infra).

Evidence for self-association in solution came from the observation that the chemical shift values of various protons present in tweezers **1**, especially those associated with the aromatic subunits, proved concentration dependent when the ^{1}H NMR spectra were recorded in CDCl$_3$ (cf. Figure 2 and Figure S1 in the Supporting Information). As can be seen from an inspection of Figure 2 and Figure S1 in the Supporting Information, increasing the concentration of **1** over the 0.5− 14.4 mM concentration range leads to upfield shifts in the signals for both the pyridine and pyrene CH resonances, with the shifts for the H$_a$ and H$_b$ resonances being particularly dramatic. In addition, the signal ascribed to the bridging
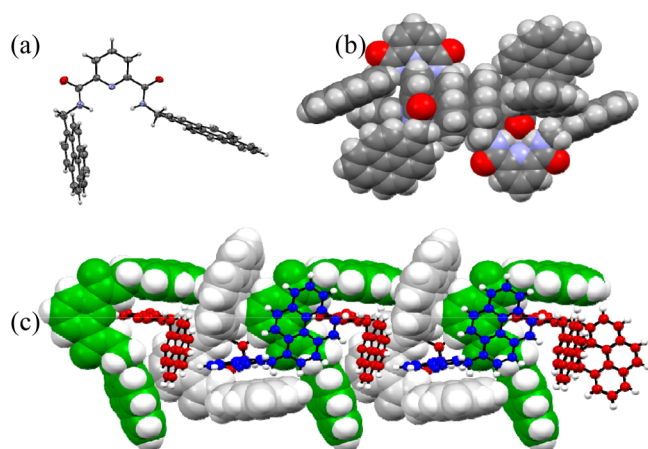
Figure 1. Views of the single crystal X-ray structure of **1** showing (a) the monomer present within the overall extended arrangement, (b) a truncated fragment found within the crystal lattice (C, gray; O, red; N, light blue; H, light gray), and (c) a more extended view of the supramolecular polymeric structure seen in the solid state.

methylene protons (H_c) shifts to higher field as the concentration of compound **1** is increased (Supporting Information, Figure S2). By contrast, the signal assigned to the amide NH protons shifts to lower field as the concentration is increased, a finding that is ascribed to an incipient intermolecular hydrogen bonding interaction between the NH protons and the carbonyl oxygen atom of another molecule.

Plots of the chemical shift changes for H_b and H_c as a function of concentration revealed no obvious breaks in what appears to be a monotonic variation (Supporting Information, Figures S3 and S4). These findings are fully consistent with a concentration-dependent aggregation process and the formation of a self-assembled structure wherein H_a and H_b are "nestled" within the tweezers-like cleft present in **1** and thus subject to the ring current effects of (at least) a nearby pyrene moiety; the result is formation of oligomeric species of varying length and size that mirror in terms of basic structure what is seen in the solid state (vide supra).[11] Similar spectral features were observed in the presence of 10% methanol-d_4 and 10%

$(CF_3)_2CHOH$ in $CDCl_3$ (cf. Figures S5 and S6 in the Supporting Information), leading us to propose that even in the presence of protic solvents compound **1** still aggregates to form self-associated supramolecular species.

The formation of self-assembled aggregated structures from compound **1** in solution was further supported by a nuclear Overhauser effect spectroscopy (NOESY) NMR study, which revealed NOE correlations between H_c and two protons of the pyrene subunit (Supporting Information, Figure S7). In addition, spectra from diffusion-ordered spectroscopy (DOSY) NMR measured at two different concentrations of compound **1** confirmed the expectation that the weight-average diffusion coefficient of **1** at a higher concentration (16 mM) was 14% smaller than the corresponding value recorded at a lower concentration (3.0 mM) (Supporting Information, Figures S8−S10). This can be taken as evidence that a more aggregated, presumably oligomeric, structure is stabilized at higher concentrations.

Consistent with its proposed supramolecular character, the self-assembled oligomer formed from compound **1** was found to undergo deaggregation with a dramatic change in structure when exposed to NAEs, such as TNB and TNT. Initial evidence for this structural change caused by TNB came from a single crystal X-ray diffraction analysis (Figure 3). Suitable crystals were obtained by allowing a dichloromethane/hexane solution of compound **1** to undergo slow evaporation in the presence of excess TNB. The resulting structure was found to be a 1:1 complex, **1**·TNB, wherein a TNB molecule is intercalated between the two pyrene subunits units that comprise the "tweezers" present in receptor **1** (Figure 3). On the basis of the observed structural parameters, this solid state TNB complex is stabilized by hydrogen bonding interactions between the NHs and one of the TNB nitro groups, as well as by apparent donor−acceptor interactions. Intermolecular $\pi-\pi$ contacts involving adjacent pyrene moieties appear to stabilize further the overall structure (Figure 3).

Further evidence for the proposed tweezers-like interactions between compound **1** and TNB and the substrate recognition-induced deaggregation of the initial self-associated form of **1** came from ^1H NMR analyses carried out in $CDCl_3$. Specifically, upon titration of **1** with TNB, the proton signals corresponding
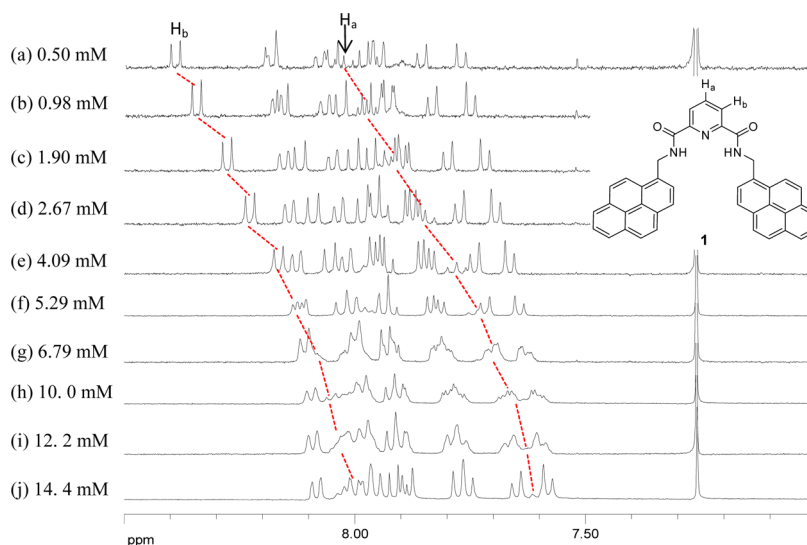
Figure 2. Partial ^1H NMR spectra of compound **1** recorded at different concentrations in $CDCl_3$.
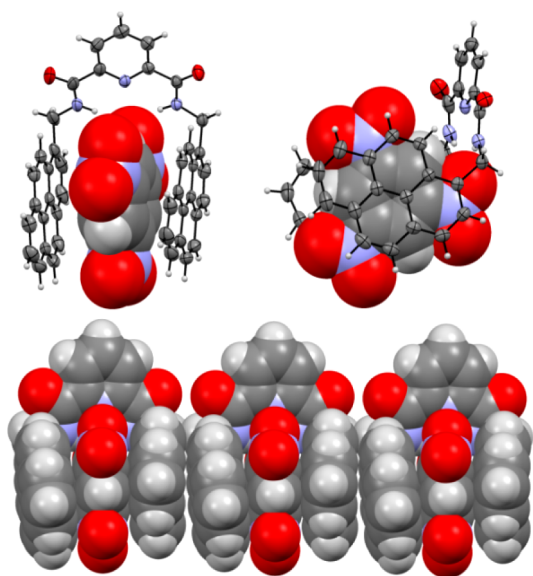
Figure 3. (top) Two different views of the donor−acceptor complex **1**·TNB as deduced from a single crystal X-ray diffraction analysis. (bottom) Partial view of the extended structure seen in the crystal lattice (C, gray; O, red; N, light blue; H, light gray).

to H_a and H_b were seen to shift to lower field (Figure 4). This finding is ascribed to the deshielding of protons H_a and H_b that results when the pyridine ring from one unit of **1** that is initially present in the tweezers-like cleft of another unit of **1** within the self-assembled form is displaced by TNB. The NH proton signals were also seen to shift to lower field during the titration, a finding that is consistent with the intermolecular hydrogen bonding interactions present in the supramoleular polymeric form of **1** being replaced by ones involving the nitro groups of the TNB bound within the complex **1**·TNB.

Coincident with the above spectral changes, the proton signals of the pyrene moiety of compound **1** were seen to shift to higher field as the concentration of TNB increased (Figure 4). Likewise, the proton signal of TNB also shifted upfield in the presence of compound **1**. For example, after the addition of 0.14 equiv of TNB to **1** in CDCl₃, the TNB proton resonance,

normally observed at $\delta = 9.40$ ppm in the ¹H NMR spectrum (Supporting Information, Figure S8), shifts to $\delta = 7.00$ ppm (Figure 4b). The changes in the TNB and pyrene signals are taken as evidence that a charge transfer complex, **1**·TNB, is formed between TNB and tweezers **1** and that this complex exists as the dominant species under most solution phase conditions (Supporting Information, Figure S11).

Similar ¹H NMR spectral changes were observed when TNB was replaced by TNT (trinitrotoluene). We thus suggest that TNT also forms a charge transfer complex with compound **1**. In both cases, the presence of the NAEs prevents **1** from forming a self-associated supramolecular polymer (Supporting Information, Figure S12). The ¹H NMR titration curves corresponding to the interaction of **1** with TNB and TNT are shown in Figure S13 in the Supporting Information. The resulting binding constants for a 1:1 interaction with **1** were determined to be 7.32×10^4 and 7.69×10^2 M⁻¹ in the cases of TNB and TNT, respectively (Supporting Information, Table S1).

The addition of TNB to a chloroform solution of **1** results in an easily discernible color change from colorless to red (Figure 5). The addition of methanol to the red solution containing **1**·
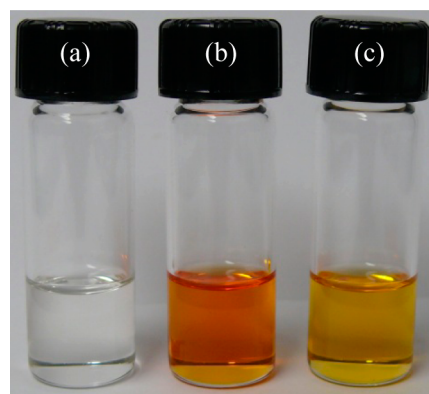
Figure 5. Color changes observed upon the addition of TNB and TNT to otherwise identical solutions of compound **1** in chloroform: (a) free **1** (1.0 mM), (b) **1** + TNB (3.0 equiv), and (c) **1** + TNT (3.0 equiv).
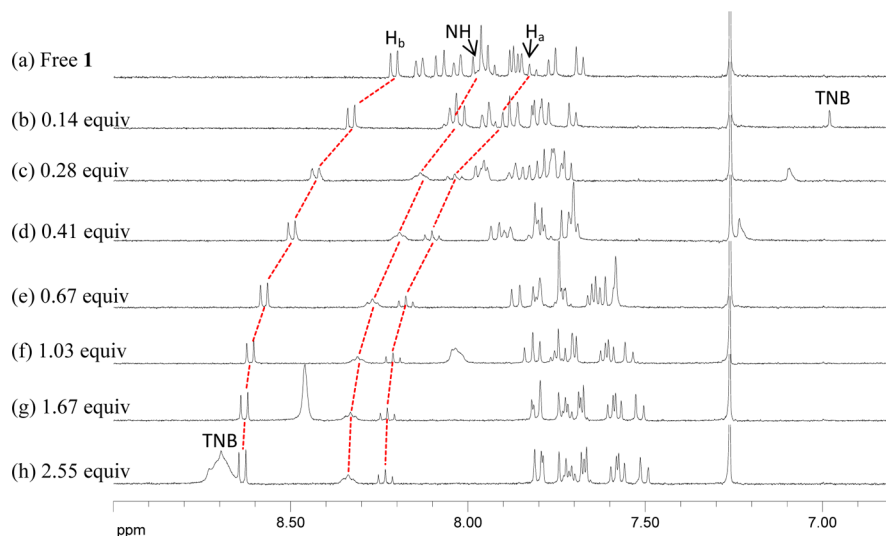
Figure 4. Partial ¹H NMR spectra corresponding to the titration of compound **1** with TNB (trinitrobenzene) in CDCl₃.

TNB leads to a loss of color (Supporting Information, Figure S14). Presumably, this latter change reflects the fact that solvation of TNB by methanol leads to decomplexation of **1**·TNB and re-formation of the supramolecular polymer formed via self-assembly of **1**. The underlying chemistry is illustrated in Figure 6 and is supported by the fact that a single crystal of **1**
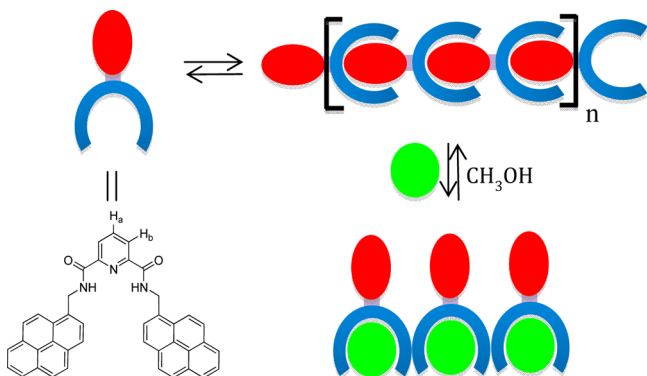
Figure 6. Schematic depiction of the supramolecular polymeric structure formed from tweezers **1** and the proposed deaggregation induced via the addition of TNB or TNT as seen in the solid state via single crystal X-ray diffraction analysis.

grown in the presence of excess TNB and methanol proved to have the same structure as crystals grown in the absence of TNB, as discussed above and presented in Figure 1.

Further evidence for the initial formation of a discrete TNB complex of compound **1** followed by deaggregation of its supramolecular polymeric structure came from NOESY and DOSY NMR spectral studies carried out in CDCl₃. In the NOESY spectrum, NOE correlations between the TNB protons and the protons of the pyrene subunits, as well as with the amide NH protons, were observed (Supporting Information, Figure S15). In the case of the DOSY NMR spectral studies (cf. Supporting Information, Figures S9 and S16), it was found that the weight-average diffusion coefficient of **1** measured (3.0 mM in CDCl₃) in the presence of TNB (2.0 equiv) was ca. 14% larger than that in its absence. At the same

time, the weight-average diffusion coefficient of the TNB guest recorded in the presence of receptor **1** was found to be ca. 6% smaller than that of TNB alone (Supporting Information, Figure S17). Taken together, these findings are consistent with the conclusion drawn above, namely that the addition of TNB or TNT to chloroform solutions of **1** leads to the formation of a discrete TNB complex and, as a consequence, serves to break up the self-assembled oligomer that would otherwise exist.

In contrast to what was seen for compound **1**, no appreciable change was seen in the ¹H NMR spectra of the phenyl linked pyrene tweezers **2** measured at different concentrations in 10% (CF₃)₂CHOH in CDCl₃ (Supporting Information, Figure S18). We take this as evidence that compound **2** does not form a supramolecular polymer under these solution phase conditions. We suggest that the difference between the phenyl tweezers **2** and the pyridine congener **1** reflects the critical role that the intramolecular pyridine N−amide NH hydrogen bonding interactions play in (1) preorganizing the two pyrene subunits to form a cleft and (2) orienting the amide carbonyl oxygen atoms outward such that they can interact with another molecule of **1**. The net result is a conformation that is predisposed to form a supramolecular polymer in the case of **1**, but not **2**.

To explore the effect of the tweezers-like nature of **1** on the formation of a supramolecular oligomer, the pyridine dipyrenemethyl ester tweezers **3** and the monopyrene amide system **4** were prepared and subject to a concentration-dependent ¹H NMR spectroscopic analysis. In these cases, no effect of concentration was seen in the ¹H NMR spectrum (Supporting Information, Figures S19 and S20). This finding provides further support for the conclusion that both NH protons in **1** are essential for stabilizing a self-associated oligomeric structure.

In order to probe the effect of the pyrene subunits on the self-assembly process observed in the case of **1**, two additional tweezers-type molecules, **5** and **6**, were prepared. These systems contain propyl groups instead of the pyrene subunits present in **1** and **2**. Proton NMR spectroscopic analyses carried out in CDCl₃ revealed that the proton signals of the amide NH protons resonate at lower field in the case of the pyridine-
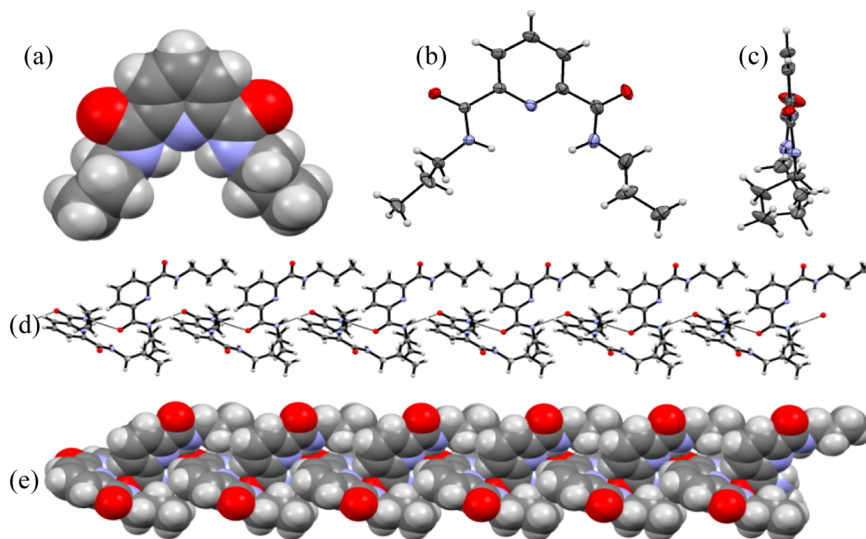
Figure 7. (a and b) Front views and (c) side view of single crystal X-ray structure of **5**. (d and e) Partial views of the extended arrangement seen in the crystal lattice (C, gray; O, red; N, light blue; H, light gray).
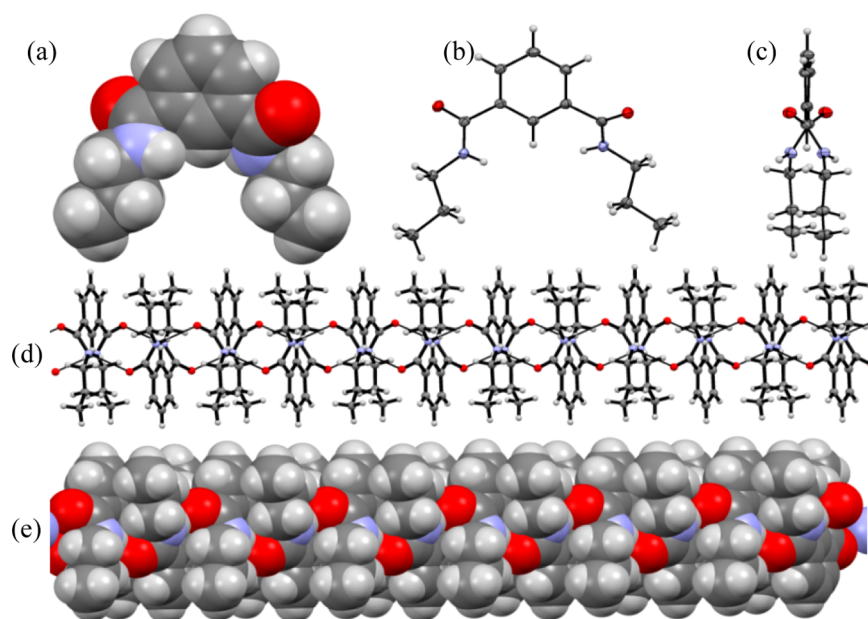
Figure 8. (a and b) Front views and (c) side view of the single crystal X-ray structure of **6**. (d and e) Partial view of the extended arrangement seen in the crystal lattice (C, gray; O, red; N, light blue; H, light gray).

containing compound **5** than they do for the phenyl-lined compound **6**. As in the cases of **1** and **2** discussed above, this difference is attributed to intramolecular amide NH to pyridine N hydrogen bonding interactions being present in **5** but not **6** (cf. Supporting Information, Figures S20 and S21). Nevertheless, for both **5** and **6** gradual downfield shifts in the proton signals of the amide NHs were observed as the concentration was increased, as deduced from ^{1}H NMR spectroscopic analyses (Supporting Information, Figures S21 and S22).

The observation of chemical shifts that change with concentration leads us to propose that both **5** and **6** self-aggregate to form supramolecular structures. Support for this contention came from single crystal X-ray diffraction studies. Single crystals suitable for these latter analyses were obtained by subjecting compounds **5** and **6** to slow evaporation from dichloromethane/methanol and water/methanol mixtures, respectively. The resulting structures, shown in Figures 7 and 8, revealed that the conformations of these two species are quite different in the solid state. In the case of compound **5**, the NH protons of the amide groups are in the same plane and are oriented toward the central nitrogen atom (Figure 7). In analogy to what was seen for compound **1**, this conformation, which appears stabilized by hydrogen bonding interactions, facilitates the formation of a "head-to-tail" supramolecular polymer. On the other hand, the two NH protons of **6** do not reside within the same plane, presumably reflecting steric repulsion from the C1 proton of the bridging phenyl ring. In fact, the two amide protons are not coplanar and point away from one another (Figure 8). Perhaps as the result of this local conformational effect, compound **6** exists in the form of a "face-to-face" supramolecular polymer in the solid state. This self-assembled arrangement appears to be stabilized entirely by intermolecular hydrogen bonds.

The self-association behavior of compound **6** inferred in solution and observed directly in the solid state stands in contrast to what was seen for compound **2** and leads us to infer that the bulky pyrene substitutents present in **2**, but not **6**, serve to inhibit self-association.

The different inter- and intramolecular interactions observed in compounds **1**−**6** in the solid state and in CDCl$_3$ led us to investigate how the inferred structural changes affected the optical properties of compounds **1** and **2**. Toward this end, the absorbance and steady state fluorescence emission spectra of **1** and **2** were first recorded in chloroform at concentrations of ca. 6 and 20 μM, respectively. As can be seen from an inspection of Figure 9, three dominant bands are seen in the absorption
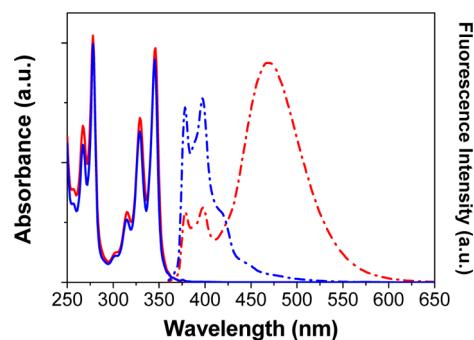
Figure 9. Normalized steady state absorption (solid lines) and fluorescence emission spectra (dotted lines) of **1** (red) and **2** (blue) recorded in chloroform. The excitation wavelength is 346 nm and the sample concentration is 20 μM, respectively.

spectra of **1** (and **2**); these appear at 316 (317), 329 (329), and 346 (346) nm, respectively. Figure 9 serves to highlight the fact that compound **2** gives rise to only pyrene monomer emission features (λ_{max} = 375 and 400 nm) when irradiated at 346 nm in chloroform. No substantial changes in these emission features were seen when other excitation wavelengths (e.g., 317 and 329 nm), corresponding to other absorption maxima, were employed. Nor was the emission spectrum found to be strongly solvent dependent, with little significant change seen when a 1:9 mixture of chloroform−methanol was employed. This stands in contrast to what is seen for **1**. Here, in addition to relatively weak monomer features, a broad structureless band
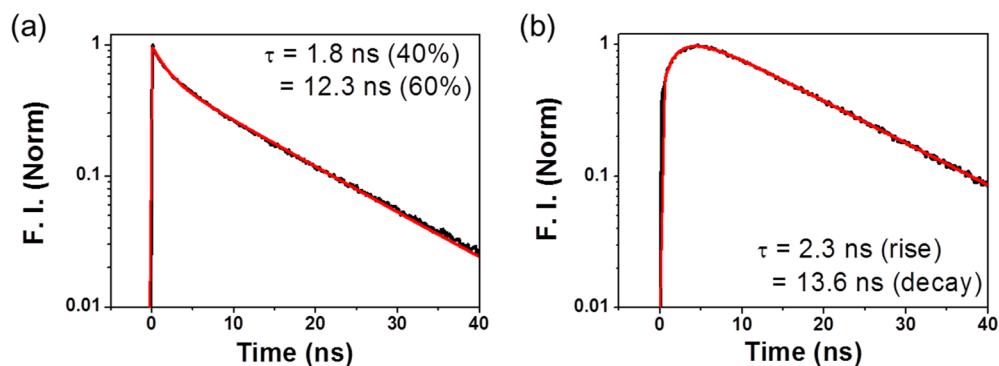
Figure 10. Fluorescence decay profiles of (a) monomer and (b) excimer emissions of **1** monitored at λ = 400 nm (monomer emission) and λ = 500 nm (excimer emission), respectively. The excitation wavelength was 355 nm and the solvent was chloroform.
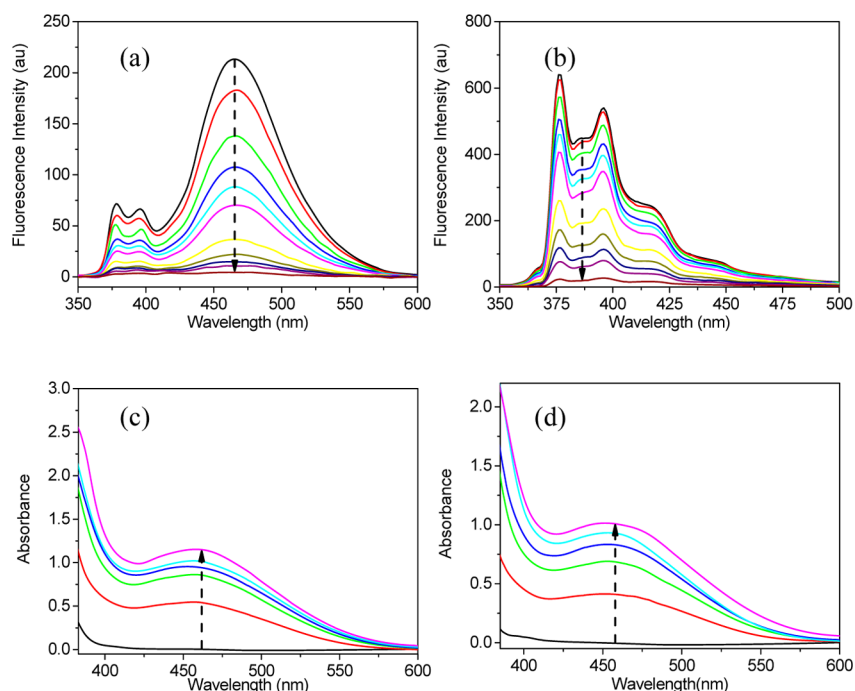
Figure 11. Fluorescence changes of (a) **1** and (b) **2** (5.0 μM, respectively) seen upon the addition of TNB (0, 10, 30, 100, 200, 300, 400, 500, 900 equiv) in chloroform with excitation at 343 nm. Also shown are the UV−vis spectra of (c) **1** and (d) **2** (1.0 mM, respectively) recorded in the presence of TNB (0, 1, 2, 3, 4, 5 equiv) in chloroform.

is seen at longer wavelengths (λ_{max} = 470 nm). On the basis of prior studies involving chemosensors having pyrene moieties, we attribute this latter feature to an excimer emission (Figure 9).[10]

Support for the emission assignments made in the cases of **1** and **2** came from fluorescence lifetime measurements carried out using time-correlated single photon counting (TCSPC). Since **1** reveals an emission feature ascribable to an excimer, along with characteristic features of a pyrene monomer, two different wavelengths regions were monitored in the context of these lifetime studies, namely 400 and 500 nm. While the excimer-derived fluorescence emission is characterized by a 13.6 ns time component, the monomer band decays with two time components (1.8 and 12.3 ns, respectively). Further, an additional rise time component of 2 ns (40%) was observed for the decay profile associated with the monomeric emission (Figure 10). We thus ascribe the 2 ns time component to excimer formation within the tweezers conformation. Very different behavior was seen for **2**. Here, only a monomer-like

pyrene emission was found. This monomer-like behavior is reflected in the fluorescence lifetime value of 7.2 ns (Supporting Information, Figure S23).

On the basis of the above observations alone, it was not possible to assign the excimer emission of **1** as originating from an intermolecular aggregate, such as observed under the conditions of the ^{1}H NMR spectroscopic analyses discussed above, or from an intramolecular excimer formation between the two pyrene moieties present in a single tweezers molecule. On the other hand, the fact that no evidence of excimer emission was seen in the case of **2** or the control compound **4** (Figure 9 and Figure S24 in the Supporting Information) led us to consider that the excimer, no matter how it was formed, was stabilized by amide−pyridine NH−N hydrogen bonds. Thus, a series of dilution and solvent polarity studies were undertaken in an effort to distinguish between these two limiting scenarios (i.e., intra- vs intermolecular excimer formation).

It was found that the ratio of fluorescence intensities (monomer emission/excimer emission) remained constant at
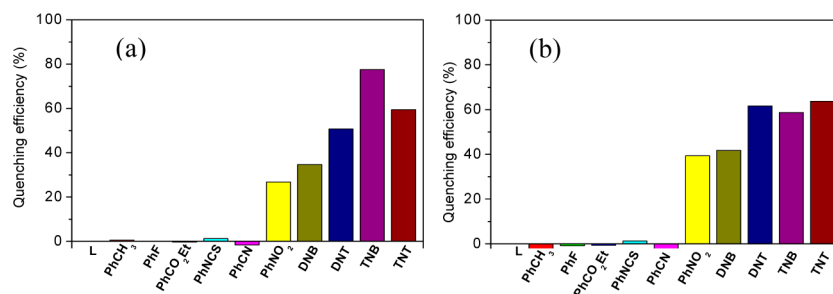
Figure 12. Relative fluorescence quenching seen for (a) **1** and (b) **2** (5.0 μM, respectively) upon addition of various guest molecules (PhCH$_3$, PhF, PhCO$_2$Et, PhNCS, PhCN, PhNO$_2$, DNB, DNT, TNB, TNT; 200 equiv of each) in chloroform. The findings are shown in bar graph form for the fluorescence intensity of the complexes (of generalized form **1**·guest) at 470 nm for under excitation at 343 nm.
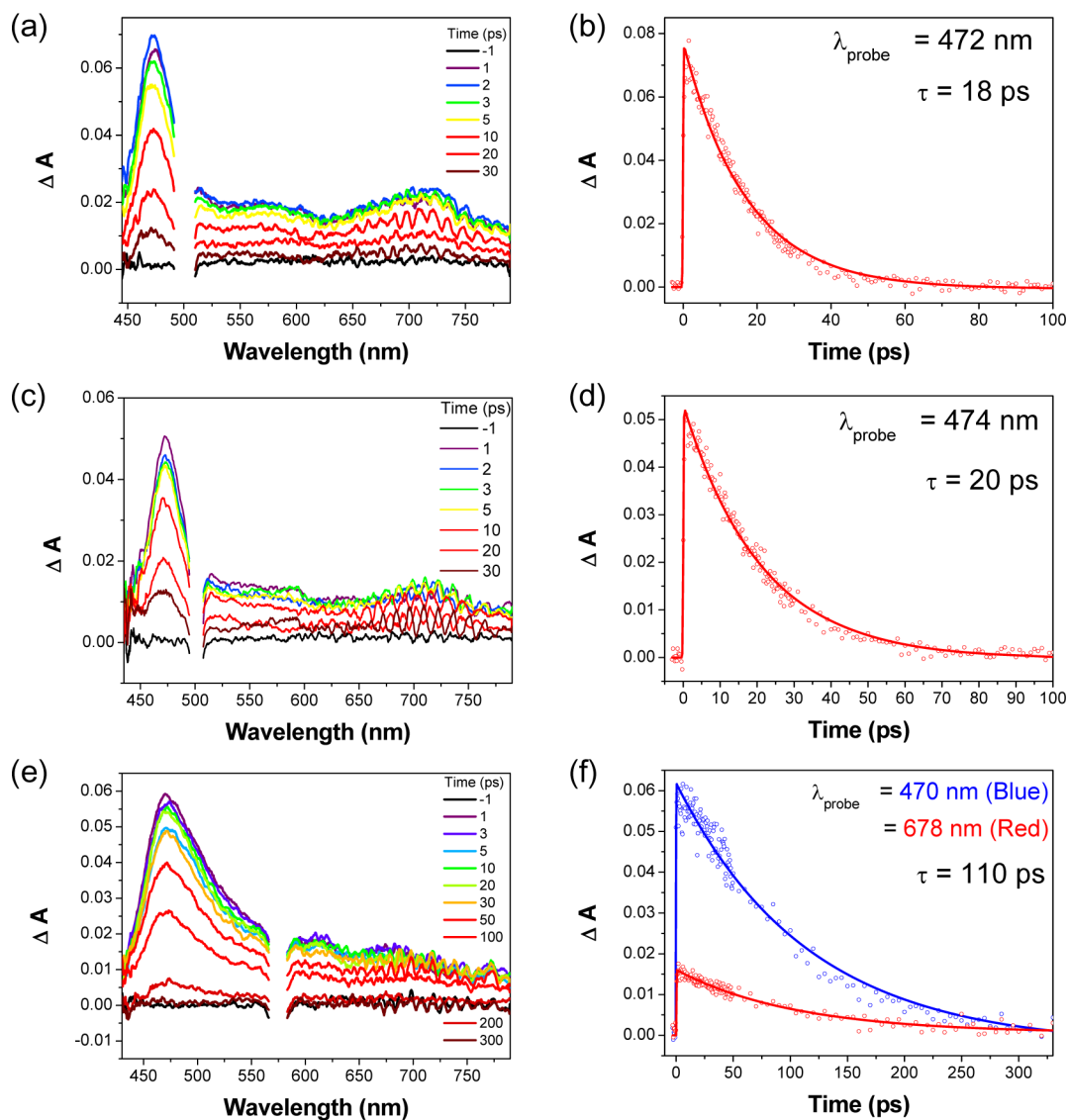
Figure 13. Transient absorption spectra and decay profiles of (a and b) **1**·TNB, (c and d) **1**·TNT, and (e and f) **1**·NT in chloroform. Excitation wavelengths are 500 and 570 nm for the TNB, TNT, and NT complexes, respectively.

different concentrations (Supporting Information, Figure S25), leading us to conclude that the excimer emission around 470 nm originates from an intramolecular interaction between the two pyrenes within the same molecule rather than an intermolecular effect.[10] This conclusion was further supported by solvent polarity studies wherein the ratio of monomer emission/excimer emission gradually increased with increasing

polarity. Such a finding is expected if, as is reasonable, the addition of methanol molecules serves to preclude the formation of intramolecular hydrogen bonds (Supporting Information, Figure S26). The absorption bands were also found to shift toward shorter wavelength with increasing polarity; presumably, this reflects decreased intramolecular

contact between the two pyrene subunits (Supporting Information, Figure S26).

Addition of TNB to solutions of **1** or **2** leads to a quenching of the fluorescence intensity. Both the monomer and the excimer-based emission intensities decrease with increasing TNB concentrations as shown in Figure 11. From the crystal structure of the **1**·TNB complex (shown in Figure 3) and the associated NMR spectroscopic analyses (vide supra), we infer that TNB "slides" into the cleft provided by the two pyrene moieties, thereby stabilizing a supramolecular donor–acceptor complex. Such a donor–acceptor complex is expected to be devoid of appreciable emission due to photoinduced charge transfer (PICT) from the pyrene moiety to TNB, as is indeed seen by experiment.

DFT (density functional theory) calculations provide support for the notion that the complexes formed between **1** and TNB are thermodynamically stable (by ~2.99 kcal/mol in the gas phase; cf. Supporting Information). For these calculations, the BSSE (basis set superposition error) was corrected via the counterpoise method.[12] These theoretical analyses are consistent with the crystallographic data, which revealed the presence of two hydrogen bonds formed between the two amide hydrogens and one of the NO_2 groups in TNB. The calculated H-bond distances are 2.21 and 2.24 Å, respectively (H-bonds are defined according to the suggested geometry cutoffs for the D−H···A hydrogen bonds,[13] i.e., H···A distances < 3.0 Å and D−H···A angles > 110°). As detailed below, experimental analyses reveal that fluorescence quenching does indeed occur in the presence of TNB.

A charge transfer (CT) band is observed around 465 nm in the absorption spectra for both **1** and **2** at higher concentrations (1 mM) in solution (as shown in Figure 11). The band (CT) intensity increases with increasing TNB concentration, and accounts for the observed color change from colorless to yellow or red (Figure 5).[9] The increase in the CT band intensity and the concurrent decrease in the excimer emission intensity with increasing TNB concentrations is consistent with the excimer being intramolecular in nature.

Several other nitroaromatic compounds, such as nitrobenzene (NB), dinitrobenzene (DNB), dinitrotoluene (DNT), and TNT, were also found to form donor–acceptor complexes with **1** and **2**. The stability of these complexes increases as the number of electron withdrawing nitro (NO_2) groups in the aromatic ring increases (Figure 12). The quenching efficiency of various aromatic compounds is summarized in Figure 12. Taken in concert, these results provide support for the conclusion that **1** and **2** differ in how they respond to electron deficient aromatic compounds. More precisely, compound **1** distinguishes mono-, di-, and trinitroaromatic compounds, whereas tweezers **2** fails to interact appreciably with any of these species. The greater efficiency of compound **1** as a recognition unit for nitroaromatic substrates is reflected in the fact that its excimer emission is easily "switched" on and off as the result of binding-induced structural changes, whereas in **2** the optical features derive almost exclusively from a monomer–monomer donor–acceptor effect.

To investigate the photoinduced excited dynamics of the proposed tweezers–electron acceptor complexes, we carried out femtosecond-transient absorption measurements (Figure 13). Upon photoexcitation of the charge transfer band at 500 nm, transient species derived from **1**·TNB and **1**·TNT are seen; these are characterized by broad excited state absorption (ESA)

features in the visible spectral region (450−800 nm) and strong ESA bands at 476 nm that are ascribed to a pyrene cation radical.[14] Consistent with the quenched fluorescence signals, the excited state dynamics of tweezers−electron acceptor complexes display relatively fast decay profiles. While the free receptor **1** displays fluorescence lifetimes on the order of 12.3−13.6 ns (vide supra), the excited state decay profiles of the complexes are characterized by relatively fast decay dynamics, namely 18 and 20 ps for **1**·TNB and **1**·TNT, respectively. These findings are taken as being indicative of complete or partial electron transfer from one of the photoexcited pyrene moieties present in **1** to the nitroaromatic guest, which acts as an acceptor.

The excited state dynamics of the present tweezers were also investigated in the presence of other electron accepting molecules, including naphthalene tetracarboxylic anhydride (NT). In the case of this latter electron deficient system, the transient dynamics of **1**·NT are characterized by spectral features similar to those seen in the case of the nitroaromatic guests. Moreover, the excited state lifetime was found to be 110 ps. On the basis of the slight differences in spectral features and excited state lifetimes seen for the various complexes, we propose that the electron transfer and charge recombination processes depend, as would be expected, on the specific choice of acceptor.

Geometry optimizations of **1**, **2**, **1**·TNB, and **2**·TNB complexes were performed for the ground state (shown in Supporting Information, Figure S27) using density functional theory (DFT) method with Becke's three-parameter hybrid exchange functional and Lee−Yang−Parr gradient corrected correlation functional (B3LYP) and the 6-31G(d) basis set. Electronic transition energies and oscillator strengths were calculated using time dependent density functional theory (TDDFT) at the B3LYP/6-31G(d) level of theory for **1** and **2**, and at the B3LYP/6-31+G(d) level of theory for **1**·TNB and **2**·TNB complexes. All the computations were carried out using the Gaussian 09 program package.[15]

The optimized structure of **1** is comparable with its crystal structure. However, the distance between the two pyrene moieties is smaller in the optimized geometry of **1** than it is in the crystal structure (~6.5 vs 7.72 Å). This could reflect the fact that solid state effects (such as polarization and intermolecular packing forces) have been neglected in the calculations. The corresponding distance in **2** (between carbon 1 of the two pyrene moieties, ~8.5 Å) is also larger than that in **1** (~6.5 Å). Formation of H-bonds (2.39 and 2.33 Å) between the amide proton and the pyridyl nitrogen in **1** is considered responsible for these differences. As noted above, such interactions are absent in **2**.

Using the optimized structure, the frontier molecular orbitals of the two tweezer systems were calculated. The results are summarized in Figure S28 in the Supporting Information. In both systems, the electron density in the highest occupied molecular orbital (HOMO) and the HOMO − 1 is mainly localized in one of the pyrene moieties. The hole density in the lowest unoccupied molecular orbital (LUMO) is confined within a pyrene moiety in **2**, whereas in **1** the hole density is delocalized through the pyrene moiety to the pyridine ring and over the whole molecule in the LUMO and LUMO + 1, respectively. The nitrogen atom in the pyridine ring plays a significant role in mediating this delocalization, as inferred from an analysis of molecular orbital coefficients.

The calculated vertical transitions of compounds **1** and **2** are summarized in Table S2 in the Supporting Information. The calculated wavelengths corresponding to the vertical excitations with the largest oscillator strengths are 343 and 345 nm for compounds **1** and **2**, respectively (Supporting Information, Table S2 and Figure S29). These wavelengths match exceptionally well with the strongest absorption peaks for both **1** and **2** (346 nm, Figure 9). However, these two tweezers molecules exhibit different features in their molecular orbital (MO) structures: while **1** exhibits electron density that extends into the bridging pyridine moiety, especially in its LUMOs, its analogue **2** reveals pyrene-localized MO features. It should also be noted that the lowest transitions of **2** are forbidden ($f < 0.01$) and consist mainly of transitions between two pyrene moieties, which show independently localized electron densities. In contrast, the lowest transitions of **1** are allowed and contain contributions from the bridging pyridine moiety.

DFT and TDDFT calculations were carried out to explore the underlying energetics associated with complex formation between tweezers **1** and **2** and the test nitroaromatic substrate, TNB. Optimized structures of the TNB complexes formed from **1** or **2** (**1·TNB** and **2·TNB**) are shown in Figure S27 in the Supporting Information. The frontier orbitals in **1·TNB** and **2·TNB** are shown in the Supporting Information, Figures S30 and S31, respectively. The HOMOs are localized on the pyrene moieties, while the LUMOs are localized only on TNB.

On the basis of the frontier orbitals, we propose that, upon photoexcitation, charge transfer occurs from the pyrene moieties to the bound TNB. This photoinduced charge transfer process (PICT) is responsible for the fluorescence quenching of **1** and **2** observed in the presence of TNB. The highest and second highest values of the calculated oscillator strengths are summarized in Table 1. The calculated wavelengths corre-

Table 1. Excitations, Oscillator Strengths, and Absorption Wavelengths in 1·TNB and 2·TNB, Calculated Using TDDFT Methods

compd	major transitions	osc strength	calcd λ (nm)
1·TNB	HOMO − 3 → LUMO	0.005	553
	HOMO −1 → LUMO + 1	0.012	831
2·TNB	HOMO − 2 → LUMO	0.004	550
	HOMO − 1 → LUMO	0.007	879

sponding to the second highest oscillator strengths match well with the observed charge transfer band (~465 nm) in the absorption spectra for these two complexes (Table 1 and Figure 11).

CONCLUSIONS

The present study has allowed a comparison between the ostensibly similar tweezers-like compounds **1** and **2**, and several control systems. As established by ^{1}H NMR spectral studies and a single crystal X-ray diffraction analysis, the pyridine-bridged tweezers **1** forms a supramolecular oligomer both in chloroform solution and in the solid state. In contrast, the close analogue **2**, which contains a phenyl, as opposed to pyridine, linker, does not. The supramolecular oligomer formed from **1** undergoes deaggregation upon exposure to TNB or TNT to form 1:1 complexes with these nitroaromatic explosives. However, the complexes are destroyed and the initial aggregated structure is re-formed upon the subsequent addition of methanol to chloroform solutions of **1·TNB** or **1·TNT**.

These transformations are accompanied by easy-to-visualize color changes. Tweezers **1** displays both pyrene monomer and excimer emissions, while **2** displays only monomer-like fluorescence features. As inferred from studies of the control compounds **3−6**, the differences between **1** and **2** are ascribed to the presence (**1**) and absence (**2**) of intramolecular hydrogen bonds between the amide NH and the pyridyl nitrogen atom. For example, in analogy to what was seen for **1**, compound **5** forms a linear supramolecular polymer in a "head-to-tail" fashion, whereas **6** self-assembles to form a "face-to-face" supramolecular polymer. This differing structural behavior is ascribed to inherent conformational differences that again reflect the presence or absence of intramolecular hydrogen bonds. This experimental finding is fully supported by theoretical (DFT and TDDFT) calculations.

ASSOCIATED CONTENT

Ⓢ Supporting Information

Synthetic procedures and spectral characterization data (^{1}H, ^{13}C NMR, and ESI mass spectra) for compounds **1−6**, binding studies, theoretical calculations, and X-ray structural data for **1** (CCDC 970248), **1·TNB** (CCDC 970249), **5** (CCDC 970250), and **6** (CCDC 970251). This material is available free of charge via the Internet at http://pubs.acs.org.

AUTHOR INFORMATION

Corresponding Author

sessler@cm.utexas.edu; jongskim@korea.ac.kr; dongho@yonsei.ac.kr

Author Contributions

All authors contributed to this work and declare no conflicts of interest.

Notes

The authors declare no competing financial interest.

ACKNOWLEDGMENTS

REFERENCES

(1) (a) Chen, C.-W.; Whitlock, H. W., Jr. *J. Am. Chem. Soc.* **1978**, *100*, 4921−4922. (b) Kamieth, M.; Burkert, U.; Corbin, P. S.; Dell, S. J.; Zimmerman, S. C.; Klärner, F.-G. *Eur. J. Org. Chem.* **1999**, 2741−2749. (c) Bryce, M. R.; Cooke, G.; Devonport, W.; Duclairoir, F. M. A.; Rotello, V. M. *Tetrahedron Lett.* **2001**, *42*, 4223−4226. (d) Klärner, F.-G.; Kahlert, B. *Acc. Chem. Res.* **2003**, *36*, 919−932. (e) Santacroce, P. V.; Davis, J. T.; Light, M. E.; Gale, P. A.; Iglesias-Sánchez, J. C.; Prados, P.; Quesada, R. *J. Am. Chem. Soc.* **2007**, *129*, 1886−1887. (f) Pérez, E. M.; Capodilupo, A. L.; Fernández, G.; Sánchez, L.; Viruela, P. M.; Viruela, R.; Ortí, E.; Bietti, M.; Martín, N. *Chem. Commun.* **2008**, 4567−4569. (g) Davis, J. T.; Gale, P. A.; Okunola, O. A.; Prados, P.; Iglesias-Sánchez, J. C.; Torroba, T.; Quesada, R. *Nat. Chem.* **2009**, *1*, 138−144. (h) Leblond, J.; Petitjean, A. *ChemPhysChem* **2011**, *12*, 1043−1051. (i) Romero-Nieto, C.; García, R.; Herranz, M.

Á.; Ehli, C.; Ruppert, M.; Hirsch, A.; Guldi, D. M.; Martín, N. *J. Am. Chem. Soc.* **2012**, *134*, 9183−9192.

(2) (a) Zimmerman, S. C.; VanZyl, C. M.; Hamilton, G. S. *J. Am. Chem. Soc.* **1989**, *111*, 1373−1381. (b) Zimmerman, S. C.; Mrksich, M.; Baloga, M. *J. Am. Chem. Soc.* **1989**, *111*, 8528−8530. (c) Zimmerman, S. C.; Saionz, K. W.; Zeng, Z. *Proc. Natl. Aacd. Sci. U.S.A.* **2009**, *90*, 1190−1193.

(3) Pérez, E. M.; Sánchez, L.; Fernández, G.; Martín, N. *J. Am. Chem. Soc.* **2006**, *128*, 7172−7173.

(4) (a) Fernández, G.; Pérez, E. M.; Sánchez, L.; Martín, N. *Angew. Chem., Int. Ed.* **2008**, *47*, 1094−1097. (b) Fernández, G.; Pérez, E. M.; Sánchez, L.; Martín, N. *J. Am. Chem. Soc.* **2008**, *130*, 2410−2411.

(5) (a) Colquhoun, H. M.; Zhu, Z.; Williams, D. J. *Org. Lett.* **2003**, *5*, 4353−4356. (b) Colquhoun, H. M. *Chem. Commun.* **2004**, 2650−2652. (c) Colquhoun, H. M.; Zhu, Z.; Cardin, C. J.; Gan, Y.; Drew, M. G. B. *J. Am. Chem. Soc.* **2007**, *129*, 16163−16174. (d) Greenland, B. W.; Burattini, S.; Hayes, W.; Colquhoun, H. M. *Tetrahedron* **2008**, *64*, 8346−8354. (e) Colquhoun, H. M.; Zhu, Z.; Cardin, C. J.; Drew, M. G. B.; Gan, Y. *Faraday Discuss.* **2009**, *143*, 205−220. (f) Zhu, Z.; Cardin, D. J.; Gan, Y.; Colquhoun, H. M. *Nat. Chem.* **2010**, *2*, 653−660. (g) Burattini, S.; Greenland, B. W.; Hayes, W.; Mackay, M. E.; Rowan, S. J.; Colquhoun, H. M. *Chem. Mater.* **2011**, *23*, 6−8. (h) Zhu, Z.; Cardin, C. J.; Gan, Y.; Murray, C. A.; White, A. J. P.; Williams, D. J.; Colquhoun, H. M. *J. Am. Chem. Soc.* **2011**, *133*, 19442−19447.

(6) Cantekin, S.; de Greef, T. F. A.; Palmans, A. R. A. *Chem. Soc. Rev.* **2012**, *41*, 6125−6137.

(7) (a) Bai, H.; Li, C.; Shi, G. *ChemPhysChem* **2008**, *9*, 1908−1913. (b) Ponnu, A.; Edwards, N. Y.; Anslyn, E. V. *New J. Chem.* **2008**, *32*, 848−855. (c) Che, Y.; Yang, X.; Liu, G.; Yu, C.; Ji, H.; Zuo, J.; Zhao, J.; Zang, L. *J. Am. Chem. Soc.* **2010**, *132*, 5743−5750. (d) Vijayakumar, C.; Tobin, G.; Schmitt, W.; Kim, M.-J.; Takeuchi, M. *Chem. Commun.* **2010**, *46*, 874−876. (e) Shanmugaraju, S.; Joshi, S. A.; Mukherjee, P. S. *J. Mater. Chem.* **2011**, *21*, 9130−9138. (f) Gole, B.; Shanmugaraju, S.; Bar, A. K.; Mukherjee, P. S. *Chem. Commun.* **2011**, *47*, 10046−10048. (g) Chen, X.; Jin, J.; Wang, Y.; Lu, P. *Chem.—Eur. J.* **2011**, *17*, 9920−9923.

(8) (a) Yang, J.-S.; Swager, T. M. *J. Am. Chem. Soc.* **1998**, *120*, 5321−5322. (b) Yang, J.-S.; Swager, T. M. *J. Am. Chem. Soc.* **1998**, *120*, 11864−11873. (c) McQuade, D. T.; Puller, A. E.; Swager, T. M. *Chem. Rev.* **2000**, *100*, 2537−2574. (d) Toal, S. J.; Trogler, W. C. *J. Mater. Chem.* **2006**, *16*, 2871−2883. (e) Tao, S.; Li, G.; Yin, J. *J. Mater. Chem.* **2007**, *17*, 2730−2736. (f) Thomas, S. W.; Joly, G. D.; Swager, T. M. *Chem. Rev.* **2007**, *107*, 1339−1386. (g) Ju, M.-J.; Yang, D.-H.; Takahara, N.; Hayashi, K.; Toko, K.; Lee, S.-W.; Kunitake, T. *Chem. Commun.* **2007**, 2630−2632. (h) Hughes, A. D.; Glenn, I. C.; Patrick, A. D.; Ellington, A.; Anslyn, E. V. *Chem.—Eur. J.* **2008**, *14*, 1822−1827. (i) Xie, C.; Liu, B.; Wang, Z.; Gao, D.; Guan, G.; Zhang, Z. *Anal. Chem.* **2008**, *80*, 437−443. (j) Zyryanov, G. V.; Palacios, M. A.; Anzenbacher, P., Jr. *Org. Lett.* **2008**, *10*, 3681−3684. (k) Germain, M. E.; Knapp, M. J. *Chem. Soc. Rev.* **2009**, *38*, 2543−2555 and references cited therein..

(9) (a) Nielsen, K. A.; Cho, W.-S.; Jeppesen, J. O.; Lynch, V. M.; Becher, J.; Sessler, J. L. *J. Am. Chem. Soc.* **2004**, *126*, 16296−16297. (b) Kim, D.-S.; Lynch, V. M.; Nielsen, K. A.; Johnsen, C.; Jeppesen, J. O.; Sessler, J. L. *Anal. Bioanal. Chem.* **2009**, *395*, 393−400. (c) Park, J. S.; Derf, F. L.; Bejger, C. M.; Lynch, V. M.; Sessler, J. L.; Nielsen, K. A.; Johnsen, C.; Jeppesen, J. O. *Chem.—Eur. J.* **2010**, *16*, 848−854. (d) Lee, Y. H.; Liu, H.; Lee, J. Y.; Kim, S. H.; Kim, S. K.; Sessler, J. L.; Kim, Y.; Kim, J. S. *Chem.—Eur. J.* **2010**, *16*, 5895−5901.

(10) (a) Winnik, F. M. *Chem. Rev.* **1993**, *93*, 587−614. (b) Kim, S. K.; Lee, S. H.; Lee, J. Y.; Bartsch, R. A.; Kim, J. S. *J. Am. Chem. Soc.* **2004**, *126*, 16499−16506. (c) Kim, S. K.; Bok, J. H.; Bartsch, R. A.; Lee, J. Y.; Kim, J. S. *Org. Lett.* **2005**, *7*, 4830−4842.

(11) (a) Lehn, J.-M. *Polym. Int.* **2002**, *51*, 825−839. (b) Ma, Y.; Kolotuchin, S. V.; Zimmerman, S. C. *J. Am. Chem. Soc.* **2002**, *124*, 13757−13769. (c) Huang, F.; Nagvekar, D. S.; Zhou, X.; Gibson, H. W. *Macromolecules* **2007**, *40*, 3561−3567. (d) Ge, Z.; Hu, J.; Huang, F.; Liu, S. *Angew. Chem., Int. Ed.* **2009**, *48*, 1798−1802. (e) Haino, T.; Fujii, K.; Watanabe, A.; Takayanagi, U. *Proc. Natl. Aacd. Sci. U.S.A.*

2009, *106*, 10477−10481. (f) Niu, Z.; Huang, F.; Gibson, H. W. *J. Am. Chem. Soc.* **2011**, *133*, 2836−2839. (g) Gröger, G.; Meyer-Zaika, W.; Böttcher, C.; Gröhn, F.; Ruthard, C.; Schmuck, C. *J. Am. Chem. Soc.* **2011**, *133*, 8961−8971. (h) Zhang, Z.; Luo, Y.; Chen, J.; Dong, S.; Yu, Y.; Ma, Z.; Huang, F. *Angew. Chem., Int. Ed.* **2011**, *50*, 1397−1401. (i) Dong, S.; Luo, Y.; Yan, X.; Zheng, B.; Ding, X.; Yu, Y.; Ma, Z.; Zhao, Q.; Huang, F. *Angew. Chem., Int. Ed.* **2011**, *50*, 1905−1909. (j) Yan, X.; Xu, D.; Chi, X.; Chen, J.; Dong, S.; Ding, X.; Yu, Y.; Huang, F. *Adv. Mater.* **2012**, *24*, 362−369.

(12) Simon, S.; Duran, M.; Dannenberg, J. J. *J. Chem. Phys.* **1996**, *105*, 11024−11031.

(13) (a) Steiner, T.; Desiraju, G. R. *Chem. Commun.* **1998**, 891−892. (b) Steiner, T. *Angew. Chem., Int. Ed.* **2002**, *41*, 48−76.

(14) (a) Richards, J. T.; West, G.; Thomas, J. K. *J. Phys. Chem.* **1970**, *74*, 4137−4141. (b) Okada, T.; Karaki, I.; Mataga, N. *J. Am. Chem. Soc.* **1982**, *104*, 7191−7195. (c) Anh, N. V.; Schlosser, F.; Groeneveld, M. M.; van Stokkum, I. H. M.; Würthner, F.; Williams, R. M. *J. Phys. Chem. C* **2009**, *113*, 18358−18368.

(15) Frisch, M. J.; Trucks, G. W.; Schlegel, H. B.; Scuseria, G. E.; Robb, M. A.; Cheeseman, J. R.; Scalmani, G.; Barone, V.; Mennucci, B.; Petersson, G. A.; Nakatsuji, H.; Caricato, M.; Li, X.; Hratchian, H. P.; Izmaylov, A. F.; Bloino, J.; Zheng, G.; Sonnenberg, J. L.; Hada, M.; Ehara, M.; Toyota, K.; Fukuda, R.; Hasegawa, J.; Ishida, M.; Nakajima, T.; Honda, Y.; Kitao, O.; Nakai, H.; Vreven, T.; Montgomery, J. A., Jr.; Peralta, J. E.; Ogliaro, F.; Bearpark, M.; Heyd, J. J.; Brothers, E.; Kudin, K. N.; Staroverov, V. N.; Keith, T.; Kobayashi, R.; Normand, J.; Raghavachari, K.; Rendell, A.; Burant, J. C.; Iyengar, S. S.; Tomasi, J.; Cossi, M.; Rega, N.; Millam, J. M.; Klene, M.; Knox, J. E.; Cross, J. B.; Bakken, V.; Adamo, C.; Jaramillo, J.; Gomperts, R.; Stratmann, R. E.; Yazyev, O.; Austin, A. J.; Cammi, R.; Pomelli, C.; Ochterski, J. W.; Martin, R. L.; Morokuma, K.; Zakrzewski, V. G.; Voth, G. A.; Salvador, P.; Dannenberg, J. J.; Dapprich, S.; Daniels, A. D.; Farkas, O.; Foresman, J. B.; Ortiz, J. V.; Cioslowski, J.; Fox, D. J. *Gaussian 09*, revision B.01; Gaussian, Inc.: Wallingford, CT, 2010.